Smart Structures and Systems, *Vol. 18, No. 4 (2016) 663-682*
DOI: http://dx.doi.org/10.12989/sss.2016.18.4.663

Modeling and control of a flexible continuum module actuated by embedded shape memory alloys

Alireza Hadi* and Hossein Akbari[a]

Department of Mechatronics Engineering, Faculty of New Sciences and Technologies, University of Tehran, North Kargar St., Tehran, Iran

(Received August 31, 2015, Revised February 4, 2016, Accepted March 24, 2016)

Abstract. Continuum manipulators as a kind of mechanical arms are useful tools in special robotic applications. In medical applications, like colonoscopy, a maneuverable thin and flexible manipulator is required. This research is focused on developing a basic module for such an application using shape memory alloys (SMA). In the structure of the module three wires of SMA are uniformly distributed and attached to the circumference of a flexible tube. By activating wires, individually or together, different rotation regimes are provided. SMA model is used based on Brinson work. The SMA model is combined to model of flexible tube to provide a composite model of the module. Simulating the model in Matlab provided a platform to be used to develop controller. Complex and nonlinear behavior of SMA make the control problem hard especially when a few SMA actuators are active simultaneously. In this paper, position control of the two degree of freedom module is under focus. An experimental control strategy is developed to regulate a desired position in the module. The simulation results present a reasonable performance of the controller. Moreover, the results are verified through experiments and show that the continuum module of this paper would be used in real modular manipulators.

Keywords: continuum manipulator; module; actuator; modeling; control; shape memory alloy

1. Introduction

Continuum manipulators are useful tools for medical robotic applications such as colonoscopy. Flexibility and maneuverability are two effective features of such manipulators. In addition, modular robotic systems are fast growing solutions in robotic applications, because the robot configuration may change quickly and easily by connecting or disconnecting different modules. Interest of modular robots due to their potential robustness, reduced costs, and wide range of application make them a suitable approach for developing continuum manipulators. In modular robots interchangeable modules are connected in a mechanical and functional assembly. Flexibility of module in shock absorption in unstructured environments is an important feature. There is a serious limitation in satisfying this requirement in regular robots.

Researchers have developed new tools for endoscopy or colonoscopy which are miniature and flexible to travel easily in restricted gap. Furthermore high consistency, precision and suitable

*Corresponding author, Assistant Professor, E-mail: hrhadi@ut.ac.ir
[a] Msc. Student, Email: hossein.akbari@ut.ac.ir

Copyright © 2016 Techno-Press, Ltd.
http://www.techno-press.org/?journal=sss&subpage=8 ISSN: 1738-1584 (Print), 1738-1991 (Online)

force control strategies help them not damage the tissues of the body (Jayender *et al.* 2009). In conventional endoscopes, the head move is managed through a control cable. This is very throbbing for the patient since control is hard to realize. Micro mechatronic technology is developing micro catheters which make the entrance to the body easier.

With the advent of shape memory alloy (SMA), continuum manipulators were developed with new properties. SMA retains the initial shape after heat transfer while a large deformation is produced in that. High power to weight ratio, low activation voltage and high biological adaptability make them a valuable actuator for medical tools.

On the other hand, smart structures may be provided using the novel properties of shape memory alloys when they are inactive. Attractive superelastic behavior of SMA was resulted in their application in developing special structures. Zhou and You (2015) investigated the SMA helical structures subjected to axial and torsional loads. Further, Salari and Asgarian (2015) worked on seismic response of steel braced frames equipped with shape memory alloy.

Through the abovementioned properties, SMAs are appropriate choices as micro catheters' actuators. Peirs *et al.* (1998) designed a shape memory actuated endoscopic tip to facilitate 180-degree turn through a modular concept. Mineta *et al.* (2001) developed a batch fabricated flat meandering shape memory alloy actuator for active catheter. Actuator was a special SMA spring manufactured of sheet through electrochemical h-pulse method and used to shrink and bend catheter head. He also developed another bending SMA actuator and attached that to a spring which resulted a one DOF active guide wire (Mineta *et al.* 2002).

A semi-automatic robot for colonoscopy was reported by Menciassi *et al.* (2002). The main intention was using the force of robot itself to move rather than using external force to push. Steering of the endoscope head was supported through three SMA springs located in a container.

Lanteigne and Jnifene (2007) developed a worm like architecture mechanical arm. Three SMA actuators was symmetrically embedded and distributed in each section of structure. Compressed warm or cold air was used to provide reverse force in the system in addition to stimulation of SMA.

Abadie *et al.* (2009) made a micro actuator using SMA bending actuators for endoscope. They increased the response time of system by assist of Peltier effect for cooling. De Sars *et al.* (2010) reported an active endoscope actuated by special SMA actuators. Special SMA springs were manufactured by laser cutting and four of them were used to develop an antagonistic mechanism. They also developed sliding mode strategy for position control of the module. In the presented works, developing a continuum manipulator has been under focus. However less attention has been made to precise control of the system.

On the other hand, producing control strategies requires a modeling platform to anticipate the behavior of system as precise as possible. Through the complex behavior of SMA, so much works was presented on modeling the material (Tanaka 1986, Liang and Rogers 1990, Brinson 1993, Gao, Qiao *et al*. 2007, Lagoudas 2008).

In addition, modeling continuum manipulators actuated by SMAs was also reported previously (Lagoudas and Tadjbakhsh 1992). The model is well verified through others (Shu *et al.* 1997, Kai and Chenglin 2007); but the model is somehow complex.

In this paper a common continuum module usable in a modular combination is considered. A modeling approach which is simple is demonstrated. Afterward an experimental based control strategy is introduced and implemented for fine regulation of position set points.

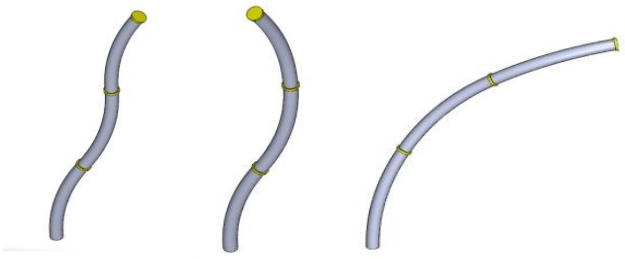

Fig. 1 A few combinations of three modules used to develop a modular manipulator

2. Actuator design

Modular robots show attractive features such as extendibility, re-configurability and easier repair and maintenance. A modular continuum manipulator consists of a few modules connected together in series. A special property which highly affects the manipulator capability is continuum deformation in contrast to classic manipulators. Deformation of every module separately, results in the change of shape of the manipulator.

Fig. 1 presents the concept of a continuum modular manipulator. Performing a common shape in the manipulator requires a predefined position in every module, which extracts from solving the inverse kinematic problem.

The focus of design in the paper is on performing an appropriate module which could be used to develop continuum manipulators. As presented in Fig. 2, structure of the module is a flexible tube of polymer with ring-shaped cross section where three SMA wires are attached to the surface in parallel. So, a differential mechanism of actuation is provided. The empty space inside the tube let electrical wires to pass through the modular manipulator.

It is observed that deflected module after activation has a consistent curvature and keep in a single plane. So, the deformed shape of module would be defined by two coordinates, θ and φ as shown in Fig. 2. As a result the module has two degrees of freedom. Because that SMA wires usually act in tension, at least three SMA wires in a differential combination were required to support the degrees of freedom.

In the straight kinematic problem of a modular continuum manipulator, the two desired parameters of θ_d and φ_d should be calculated for every module. In this paper, the control problem of a single module is under focus, but the results will be used in the future work to set a defined position of the continuum manipulator.

An important feature of the module is controllability of deformation. Feedback system is very effective and supports the closed loop control. Especially this is more important for the SMA actuated mechanisms where the model is not reliable. However, the sensory system should be as small as possible for miniaturizing the manipulator. Embedding sensors in the body of the module is a way but makes the design complex.

Measuring orientation of module's end plate and extracting the module deflection from that is the way used in this research. So, a tilt sensor is mounted on the end plane of the module and a conversion is used to transform measured inclination data into deformation parameters, φ and θ.

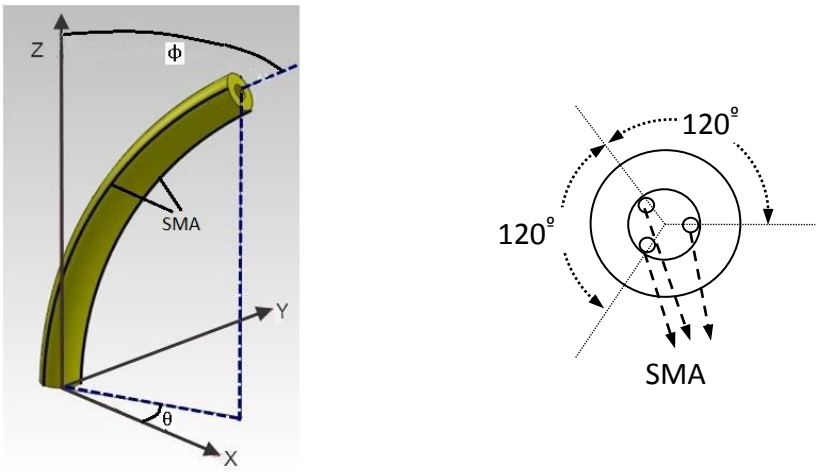

Fig. 2 General concept of the flexible SMA-actuated module

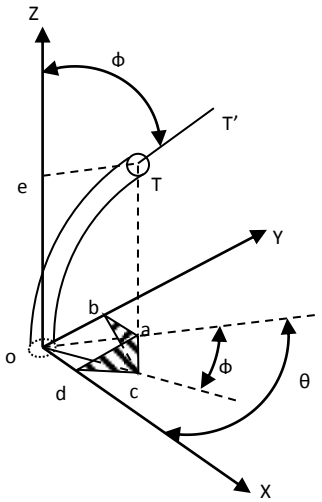

Fig. 3 Relation of tilt angles and module geometric parameters

For transformation of end plate inclination into φ and θ, the set of Eq. (1) is extracted using Fig. 3. In Fig. 3 line $\overline{oa}$ shows the projection of module on xy plane. In addition, points d, b and e represent the coordinates of module tip on axis x, y and z respectively. θ_x is the angle between line $\overline{da}$ and $\overline{dc}$ in the triangular Δadc while θ_y is defined by the angle between lines $\overline{ba}$ and $\overline{bc}$ in the triangular Δabc. It should be noted that in Fig. 3 the angle between TT′ and Z axis in addition to the angle between two lines $\overline{oa}$ and $\overline{oc}$ is φ. Considering the two triangular Δabc and Δadc in Fig. 3, Eq. (1) would be concluded as

$$\begin{cases} for\ \theta = \dfrac{\pi}{2} : \varphi = \theta_x \ and\ \ for\, \theta = 0 : \varphi = \theta_y \\ if\ \ \theta \neq \dfrac{\pi}{2} : \tan(\theta_y) = \dfrac{\tan\varphi}{\cos\theta} \\ if\ \ \theta \neq 0 \Rightarrow \tan(\theta_x) = \dfrac{\tan\varphi}{\sin\theta} \end{cases} \tag{1}$$

So, if $\theta \neq 0$ and $\theta \neq \pi/2$, using Eq. (1), we have

$$\theta = \tan^{-1}\left(\frac{\tan\theta_y}{\tan\theta_x}\right) \tag{2}$$

Calculating θ from Eq. (2), φ was extracted from Eq. (1).

3. Modeling

The goal of modeling in this paper is anticipating deflection of the module after activation of SMAs. In this way the model of SMA would be added to the model of flexible structure of the module.

One of the suitable methods in defining the SMA behavior is constitutive models. Tanaka (1986), Liang and Rogers (1990), Brinson (1993) and Gao *et al.* (2007) presented the most famous constitutive models developed during 1986 to 2007. Brinson constitutive model, which is more capable to define complex loading of SMA, is described by

$$d\sigma = Ed\varepsilon + \Omega d\xi_s + \Theta dT \tag{3}$$

where σ is the stress, E represents the young modulus, ε indicates the strain, Ω is the phase transformation contribution factor, ξ_s is the de-twinned martensite fraction, Θ defines the thermal expansion and T represents the temperature of the SMA.

Through the enhanced model of Brinson for phase transformation (Gao *et al.* 2007), martensite fraction would be defined by

$$\xi = f(\sigma, T) \tag{4}$$

where ξ stands for martensite fraction. The temperature in above equations would be extracted of the heat transfer model of each SMA which defined by

$$mc_p \frac{dT}{dt} + mL\dot{\xi} = \frac{V^2}{R} - h_c A_c (T - T_\infty) \tag{5}$$

where m is the mass, c_p is specific heat, L is the latent heat factor, V is the voltage, R is the electrical resistance, h_c is the convection heat coefficient, A_c is the circumferential area of convection and T_∞ stands for environment temperature.

Another relation is required to be coupled with Eqs. (3)-(5) for extraction of four unknown states in Eq. (3). The relation would be defined using the kinematics and dynamics of the system which is discussed in the following.

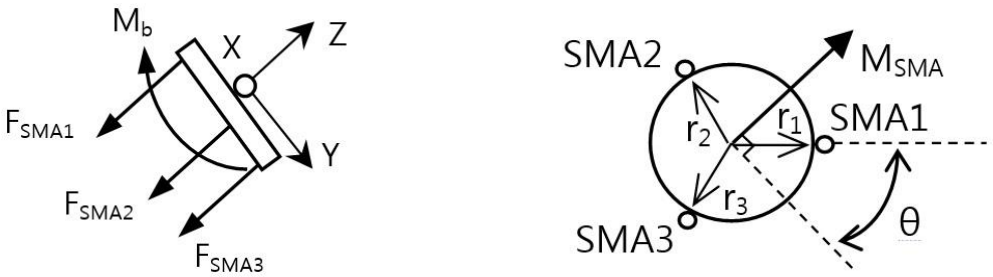

(a) Free body diagram of the rigid plate mounted at the end of module

(b) The resultant moment of SMAs in every cross section of module and relation of θ with that

Fig. 4 The loading of the module

In the module, three shape memory alloy actuators produce a loading on the flexible tube which bends the module after activation. The loading is substituted by a resultant force and moment act on the tube. As shown in Fig. 4(a), in the free body diagram of the module end plate, M_{SMA} defines the resultant moment of SMA forces on end plate and M_b is the opposing moment of the tube against bending.

In this paper, a simple model for defining the module deflection is considered (Hadi 2012). Because of the slow response of SMAs, the dynamic of system is not under focus. So, it is assumed that module is bent the by resultant moment M_{SMA}. So, the module bend in a plane which M_{SMA} is the normal vector. Consequently, as shown in Fig. 4(b), the line represents the angle θ is always perpendicular to M_{SMA} vector.

From the free body diagram of module's end plate, as shown in Fig. 4(a), Newton's second law along the main axis of the plate is defined by

$$(M_{SMA})_x - M_b - c\dot{\varphi} = I\ddot{\varphi} \tag{6}$$

where I indicates the moment of inertia and c stands for the damping constant.

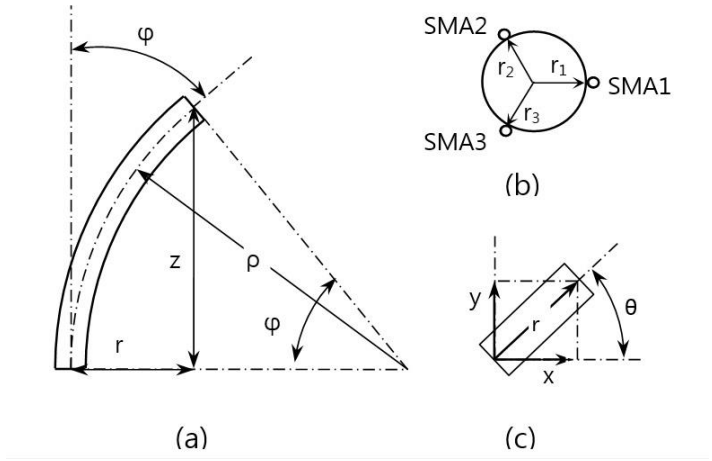

Fig. 5 Module geometry

Strain of each SMA in Eq. (3) would be performed if we know SMA length. The length of each SMA is related to module deformation. It means that by extracting module deformation by measuring φ, the SMA length is performed by inverse kinematic problem of the module. From the geometry of the module illustrated in Fig. 5, the lengths of SMAs in addition to other kinematic parameters are calculated by Eq. (7) as

$$\begin{aligned} x &= r\cos\theta \\ y &= r\sin\theta \\ z &= \rho\sin\varphi \\ r &= \rho - \rho\cos\varphi \\ l_i &= (\rho - r_i\cos(\theta_i))\times\varphi \end{aligned} \tag{7}$$

Through the observation of the manufactured module, it was concluded that the curvature of the module after activation do not change so much along the module length. So, using strength of material for a beam under absolute bending, the curvature is constant along the beam length and would be calculated by

$$\frac{1}{\rho} = \frac{M_b}{EI} \tag{8}$$

Using Fig. 5, the following kinematic relation is realized

$$\rho\varphi = l \tag{9}$$

Substituting Eq. (9) into Eq. (8), Eq. (6) was rewritten by

$$M_{SMA} - \frac{EI}{l}\varphi - c\dot{\varphi} = I\ddot{\varphi} \tag{10}$$

4. Simulation

Simulink environment in Matlab software was a choice for simulating such a system (Hadi *et al.* 2010). The general scheme of the system modeling is presented in Fig. 6. Constitutive model, heat transfer, phase transformation, module dynamic and module kinematics are the Sub-models of the whole model. The parameters of modeling and simulation are presented in Table 1.

However, by increasing the quantity of SMA actuators and adding the controller, the complexity of the nonlinear system increases too much. Although the differential form of Eq. (3) was a better choice in simulation rather than the integral form, it would be concluded that Simulink wasn't an efficient tool to solve the problem. Consequently, the composite model was implemented through a programming code.

For modeling verification, a set of experiments is designed and employed. In the simulation and the experiment, the SMAs are actuated and variations of module parameters θ and φ are evaluated. In Fig. 7, the SMA1 is activated with 2.6 V for 50 s while Fig. 8 illustrates the variation of φ when the SMA3 is activated with 2.6 V for 50 s. In the first experiment, parameter θ is consistently equal to 0 and consequently its variation is not reported.

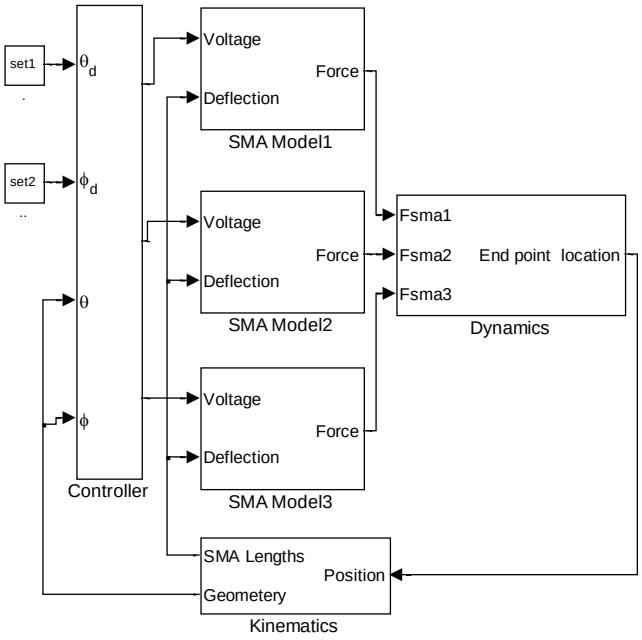

Fig. 6 Block diagram of the whole module dynamic model

Table 1 Coefficients used in the modeling

Coefficient	Definition	Value	Unit
R_A	SMA resistance in austenite phase	1.4	Ω
R_M	SMA resistance in martensite phase	1	Ω
h	Convection heat coefficient	150×10^{-6}	J/m2 ˚Cs
C_p	Specific heat of SMA	840	J/kg◦C
r	SMA mounting distance from module center	3	mm
C_A	Effect of stress on austenite temperatures	6	˚C
C_M	Effect of stress on martensite temperatures	6	˚C
d	Diameter of SMA wire	0.38	mm
L	Latent heat	6025	J/kg˚C
m	SMA spring mass	0.73×10^{-6}	Kg/mm
l_0	SMA minimum length	100	mm
l	module length	100	mm
l_i	SMA initial length	104	mm
y_L	Maximum recoverable length of SMA wire	106.7	mm
E_A	young module of SMA in austenite	75	GPa
E_M	young module of SMA in martensite	28	GPa
E_b	young module of elastic tube	25	MPa

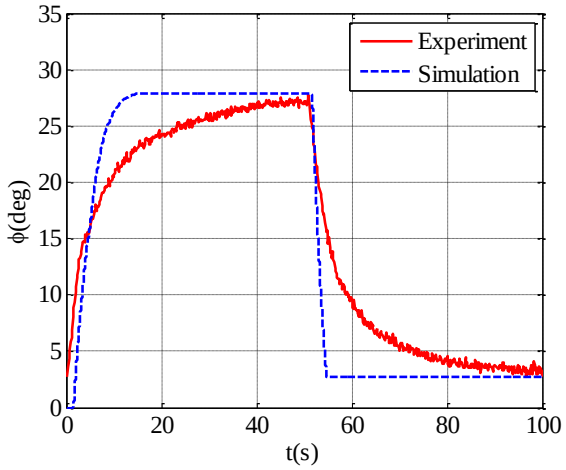

Fig. 7 Variation of φ when activating the SMA1 with 2.6 V for 50 s

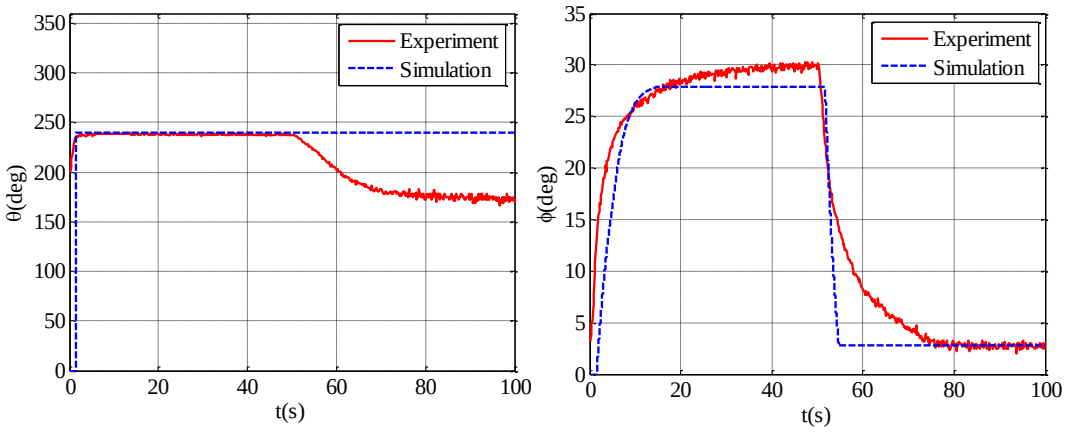

Fig. 8 Variation of φ when activating the SMA3 with 2.6 V for 50 s

Through the presented figures, the model generally perform the module behavior, however, there exist some deviations. This deference is due to a few reasons. Firstly, initial conditions of the SMAs may not be the same before activation. Secondly, the heat transfer model of the system may not be exact. As the third reason, the manufactured module parameters may not be the same as the design used in simulation. In Fig. 8, θ changes in experiment by deactivating the SMA2 while no variation is reported for that in the simulation. It should be noted that, in the simulation, the effects of the other totally deactivated actuators are considered the same, while they may not exactly be identical in reality. In this experiment, the force of the SMA2 is greater than that of the SMA1 in deactivation phase, which causes deviation in position after about 50 s.

5. Control

In the paper, the control problem focuses on regulation of module deformation described by two set points: φ_d and θ_d. The challenge of the controller is simultaneous control of the both parameters. Complex behavior of SMA, make the control problem hard. Because of that, in many SMA-actuated systems, the actuators are utilized only in ON or OFF mode. In contrast, here a common set point was provided by regulating the amount of all SMAs' activation.

On one hand, through the nonlinear and non-repeatable properties of shape memory alloys, variable structure control (VSC) is a proper candidate as a control strategy (Ashrafiuon and Jala 2009). Sliding mode control (SMC), as a kind of VSC, is a powerful strategy for implementing in nonlinear systems with uncertain model. So, for the module of this paper, the aforementioned strategies are suitable choices to be applied.

On the other hand, in sliding mode control, all states of the system should be known (Ashrafiuon and Jala 2009). Calculating or measuring states like stress, temperature and martensite fraction is not simple. Consequently, although sliding mode is a proper choice for such a system, requiring all the states is a challenge in real implementation of that. Developed control strategy in this paper does not require stress and temperature.

Through the value of θ_d, the control strategy categorizes the problem into three regions. In each one, only two SMAs are required to be active and the other one action is passive. The three regions in addition to active and passive SMAs in the regions are reported in Table 2.

The control algorithm of the module is illustrated in Fig. 9. In the algorithm, a major loop is run which guide θ to θ_d. Further, through a minor loop the algorithm tries to near φ to φ_d. In every loop, using Table 2, active SMAs are selected. Table 3 presents the VSC rule of controlling θ in the major loop. The logic of the rules is based on the fact that for a desired value of θ_d, regard to its region, one of the active SMA increases the theta while the other active SMA decreases that. For example in the first area, increase of SMA1 voltage decreases the θ while adding the voltage of SMA2 tends to the θ increase. Consequently, using such a rule in every region, through a set of switching around the set point, the θ_d is realized.

Table 2 Active and passive SMAs in every regions

Region	θ_d range	Active SMAs	Passive SMA
1	$0^o < \theta_d < 120^o$	SMA1 and SMA2	SMA3
2	$120^o < \theta_d < 240^o$	SMA2 and SMA3	SMA1
3	$240^o < \theta_d < 360^o$	SMA1 and SMA3	SMA2

Table 3 VSC rule of control θ in different areas

Region	VSC rule
1	If $\theta < \theta_d$: SMA1 is OFF, SMA2 is ON If $\theta > \theta_d$: SMA1 is ON, SMA2 is OFF
2	If $\theta < \theta_d$: SMA2 is OFF, SMA3 is ON If $\theta > \theta_d$: SMA2 is ON, SMA3 is OFF
3	If $\theta < \theta_d$: SMA1 is ON, SMA3 is OFF If $\theta > \theta_d$: SMA1 is OFF, SMA3 is ON

The logic for nearing φ to φ_d, is based on the fact that stimulating both active SMAs of a region, increases the φ while deactivating both one, decreases the φ. Table 4 presents the VSC rules for control of φ. Using this fact, the activation voltage of SMAs is set in every control loop to settle θ_d in addition to φ_d.

In the algorithm of Fig. 9, the effective activation voltage is determined by assigning a duty cycle for every active SMA. This property of a digital controller could be implemented through a simple hardware. The assigned percentage of duty cycle in the algorithm is 0% for making the actuator off or 100% for making the actuator on. V_{set} stands for the activation voltage. However, by changing the duty cycles assigned in the algorithm, better results may be provided. More discussion about the results is presented in section 7.

To enhance the control strategy, a new rule similar to PD controller was added to the control strategy. The rule utilizes error rate in addition to error to choose active SMA. The new rule is defined as

$$\text{If} \quad \varphi_d\text{-h}<\varphi<\varphi_{d+}\text{h and} \quad (d\varphi/dt)>0 \quad \text{Then SMAi,j=off}$$

$$\text{If} \quad \varphi_d\text{-h}<\varphi<\varphi_{d+}\text{h and} \quad (d\varphi/dt)<0 \quad \text{Then SMAi,j=on}$$

However in the above rule, making the actuator on or off would be through a common duty cycle not exactly 0 or 100. The enhanced algorithm is presented in Fig. 10.

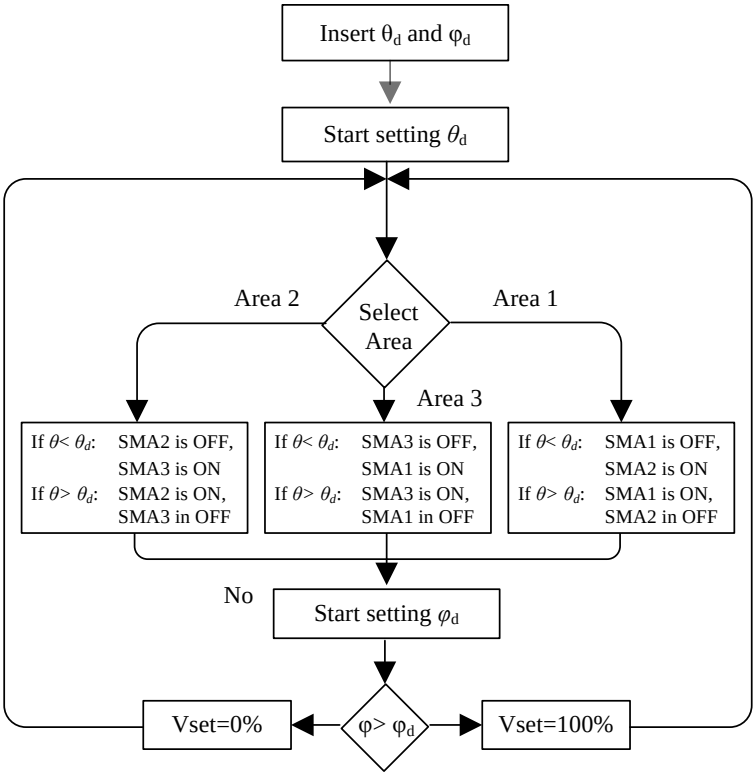

Fig. 9 The Position Control Strategy of Module

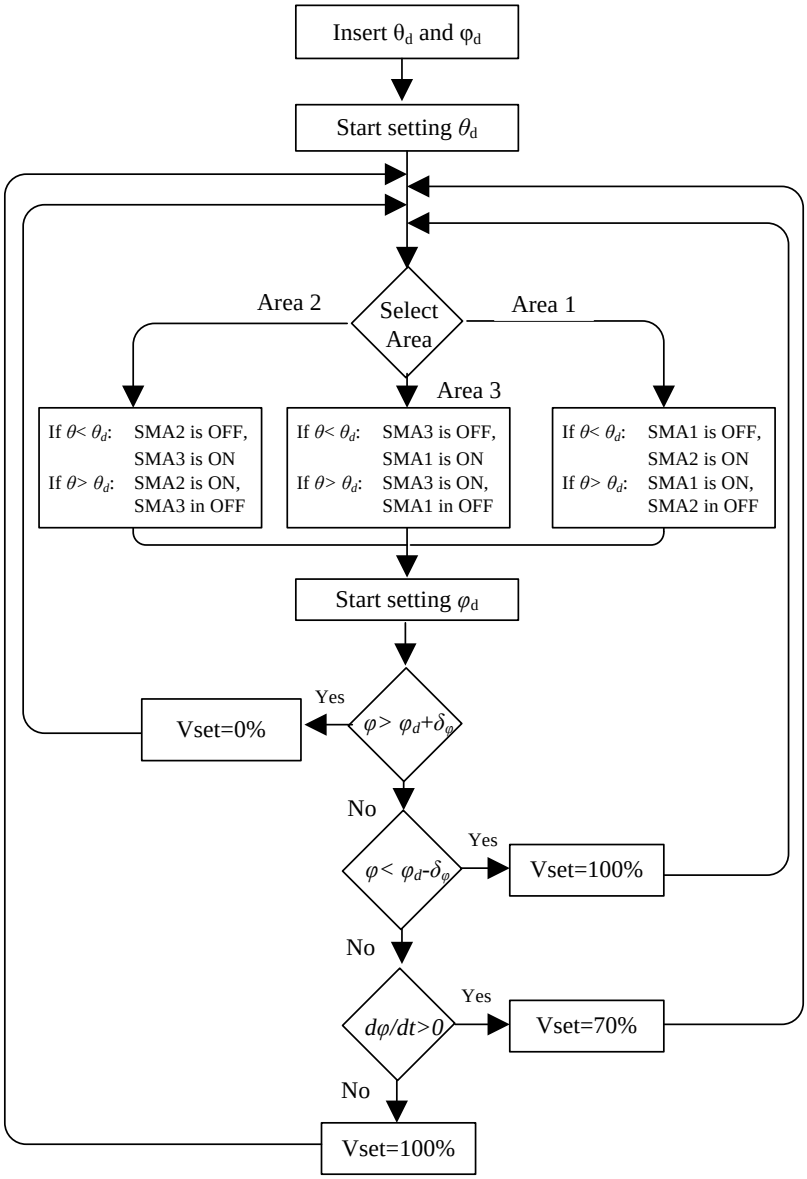

Fig. 10 The enhanced position control strategy of module

A way for presenting the performance and convergence of the controller is using the phase plane trajectory of system. In this way the following relations are defined and used in section 6 for evaluation of the algorithm

$$e_\theta = \theta - \theta_d,\ \dot{e}_\theta = \dot{\theta} - \dot{\theta}_d$$
$$e_\varphi = \varphi - \varphi_d,\ \dot{e}_\varphi = \dot{\varphi} - \dot{\varphi}_d \tag{9}$$

Table 4 VSC rules of control φ in various regions

Region		VSC rule
1	If $\varphi < \varphi_d$:	SMA1 is ON, SMA2 is ON
	If $\varphi > \varphi_d$:	SMA1 is OFF, SMA2 is OFF
2	If $\varphi < \varphi_d$:	SMA2 is ON, SMA3 is ON
	If $\varphi > \varphi_d$:	SMA2 is OFF, SMA3 is OFF
3	If $\varphi < \varphi_d$:	SMA1 is ON, SMA3 is ON
	If $\varphi > \varphi_d$:	SMA1 is OFF, SMA3 is OFF

6. Experiment

Through the modeling relations, a suitable geometry for the module may be selected. SMA force and strain in addition to flexible tube length and strength are the parameters affect the maximum deflection of the module. A common size for the test bed of this paper is selected as 11.5 mm in diameter and 100 mm in length. Also the tube includes a hole with 5.5 mm diameter. However, the geometry would be scaled to smaller sizes for real applications.

The experimental setup of the experiment is presented in Fig. 11. For measuring the orientation of module end plate, an inclination sensor was utilized and mounted on that. The inclination sensor was ZCT-260 with accuracy of 1º. The measured angles, which are rotation around x and y axis of the sensor, were sent continuously to control board through serial communication. The control board was micro controller based. Power transistors were used to drive the SMA actuators.

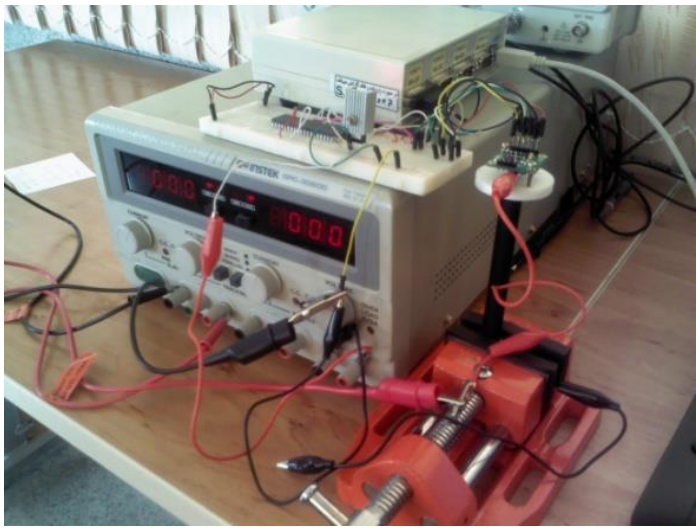

Fig. 11 The hardware setup

7. Results and discussion

The modeling equations extracted in section 2 in addition to simulation platform described in section 3, were used to implement the control strategy discussed in section 5. At first, the control strategy described in Fig. 9, without any boundary layer around φ_d, is applied and the generated results through simulation are presented in Fig. 12. In the strategy, the major control loop is positioning the position θ. So, as seen in the Fig. 12, θ_d is tracked reasonably while φ_d is not tracked as well. Oscillations with a large overshoot was observed around the set point position φ_d.

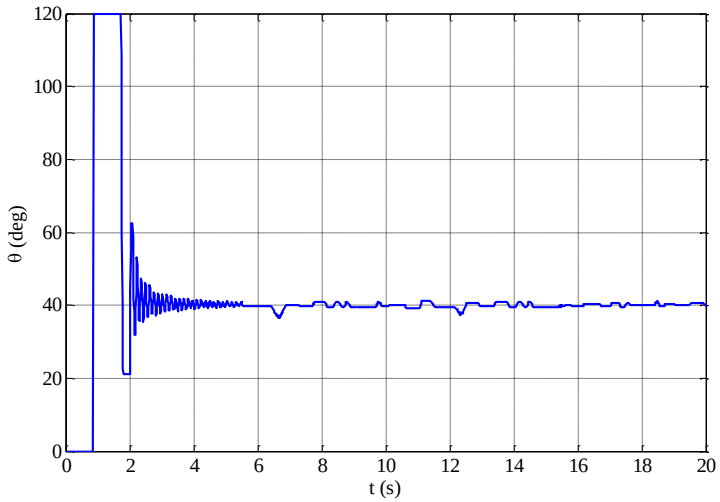

(a) θ versus time

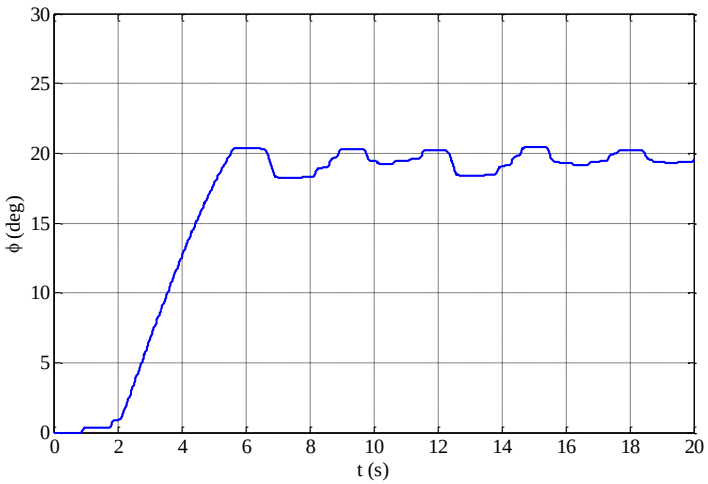

(b) φ versus time

Fig. 12 Controller results for θ_d=40°, φ_d=20°, without boundary layer arround φ_d (Simulation)

A better result was reported by varying the duty cycle of SMA for OFF state in the algorithm. As shown in Fig. 13, by setting the duty cycle of OFF state to 60% instead of 0%, the overshoot and steady state error was improved, but φ is still varying around the set point φ_d.

The results of applying the enhanced control strategy in simulation are shown in Fig. 14. As seen, a better steady state error of φ with less oscillation is provided. In the following the enhanced control algorithm is applied to evaluate the policy in experiment.

The width of the defined boundary around the set point φ_d, influences the steady state error of position. In fact by increasing the boundary width, steady state error becomes larger, although the controller would be more robust against the disturbance. Because in a narrow boundary, any disturbance remote the module position form φ_d easier. As in the algorithm the priority of control is the θ state, deviation of φ is reported higher than θ. Consequently, with a more disturbance in the environment, the algorithm requires a bigger boundary width. In this paper, without any disturbance, the value of boundary in the simulation as Fig. 14 is set to 0.5°. However, to guarantee a more robustness, in experiments it is set to 2°.

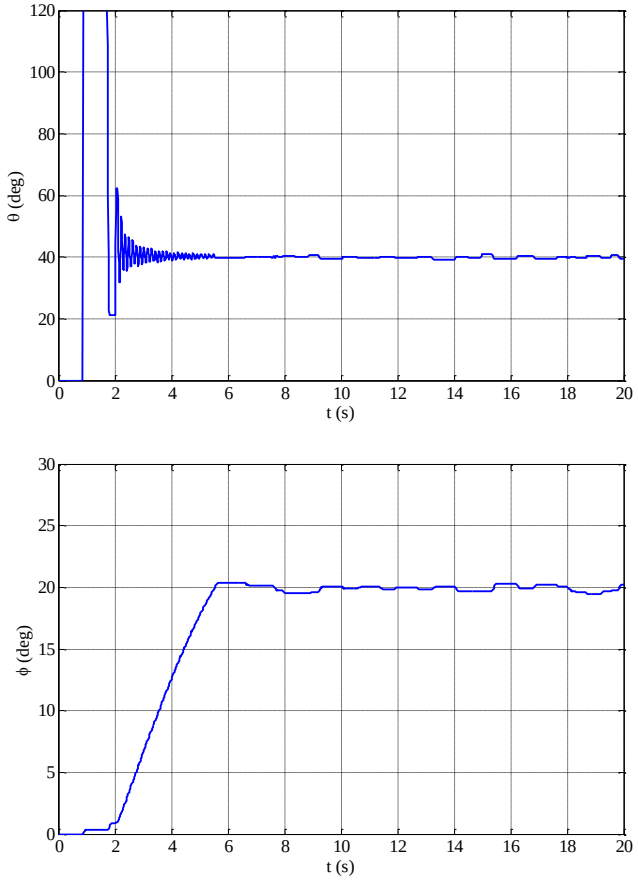

(b) φ versus time

Fig. 13 Controller results for θ_d=40°, φ_d=20°, with boundary layer around φ_d (Simulation)

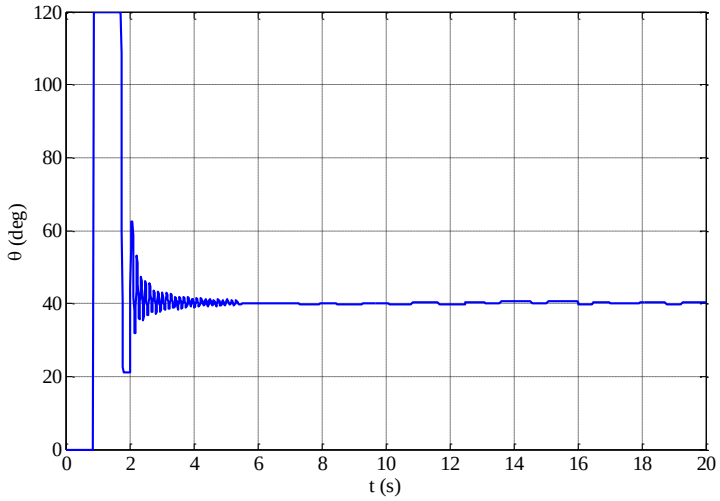

(a) θ versus time

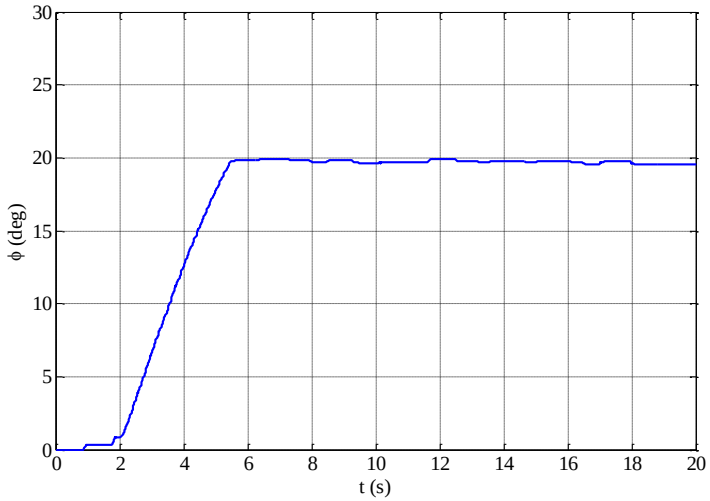

(b) φ versus time

Fig. 14 Controller results for θ_d=40°, φ_d=20°, using the new rule considering the error rate (Simulation)

Another parameter of the control strategy which affects the controller performance is V_{set} value. In fact by increasing the activation voltage, the response of the actuator would be faster. But as the SMA may be broken through overheat; we should consider a safe voltage in the algorithm. Also the change of the effective voltage is provided by changing the duty cycle of activation.

The phase plane trajectory of module is presented in Figs. 15 and 16. Using the Eq. (9), trajectories are produced in the phase plane of $\dot{e}$ versus e.

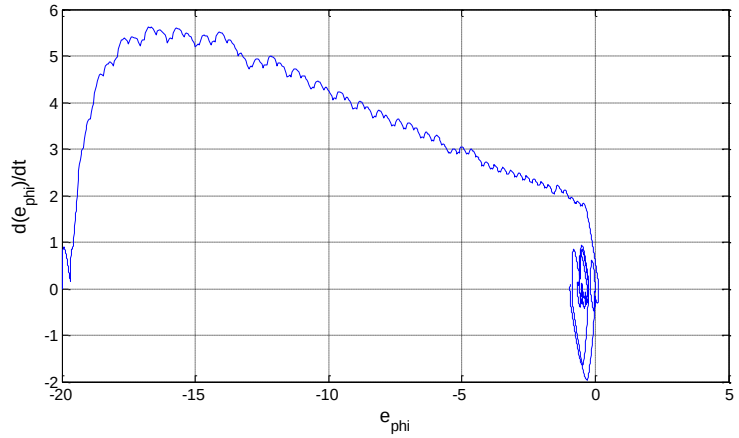

Fig. 15 Phase plane trajectory of module in φ plane (Simulation)

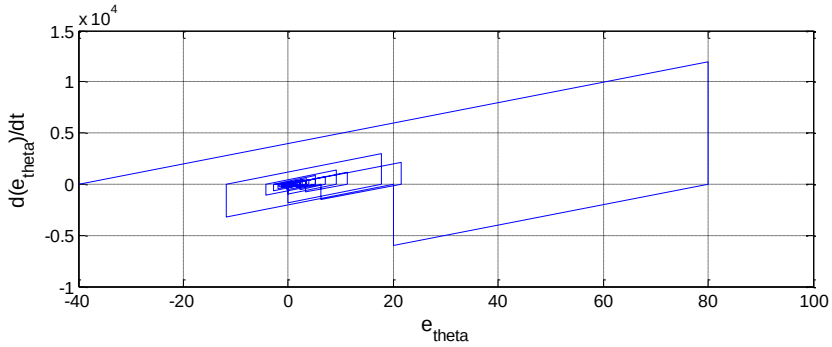

Fig. 16 Phase plane trajectory of module in θ plane (Simulation)

To validate the control plan, a set of experiments was employed. The results for different set points in the workspace are illustrated in Figs. 17-19. Using the Table 2, the workspace is divided into three regions regard to the value of set point. In Fig. 17 the set point is selected as φ_d=10° and θ_d=300° which is in third region; while in Fig. 18 the set point is located to φ_d=30° and θ_d=160° which is in the second region. Also, in Fig. 19 the set point is placed at φ_d=20° and θ_d=140° which is in the second region.

As illustrated in the results of experiment, the control strategy utilized for the continuum module supplies a reasonable position error in a regulation problem.

8. Conclusions

In this paper modeling and control of a flexible module usable in developing modular continuum manipulators was studied. A typical size of module was investigated in this paper.

However, the system is capable to be developed in more miniature sizes. Moreover the biological compatibility of shape memory alloys enhances the usage in medical applications.

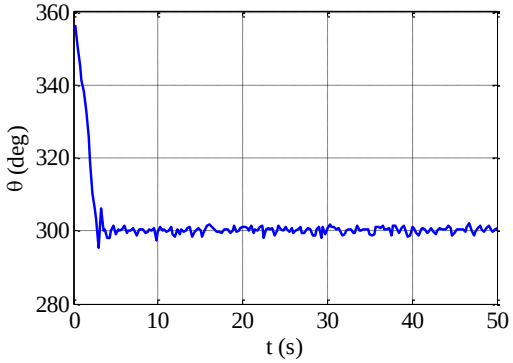

(a) θ versus time

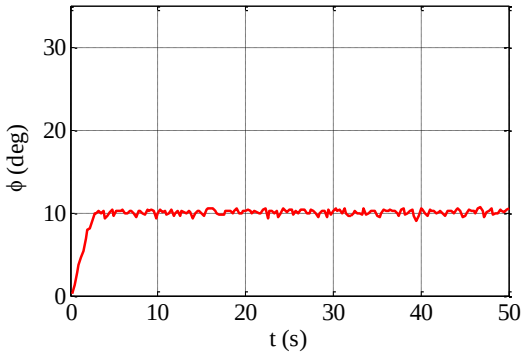

(b) φ versus time

Fig. 17 Variation of position for φ_d=10° and θ_d=300° (Experiment)

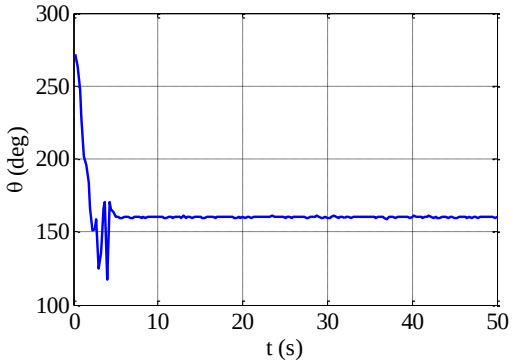

(a) θ versus time

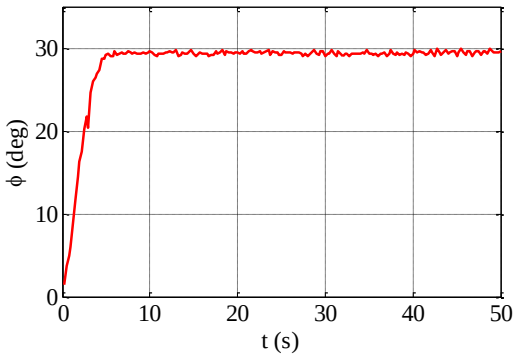

(b) φ versus time

Fig. 18 Variation of position for φ_d=30° and θ_d=160° (Experiment)

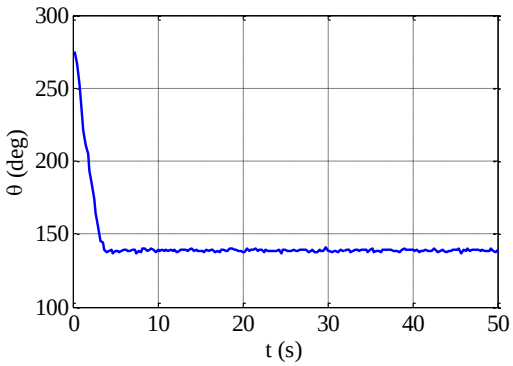

(a) θ versus time

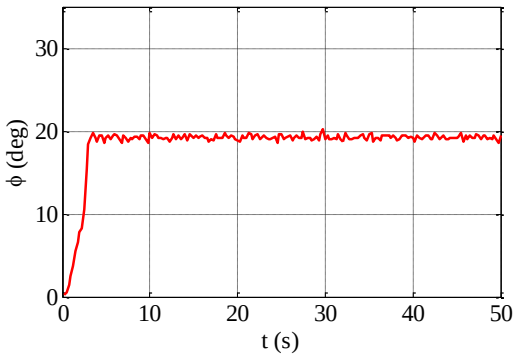

(b) φ versus time

Fig. 19 Variation of position for φ_d=20° and θ_d=140° (Experiment)

In many devices were developed by SMA actuators the SMA stimulation is only ON or OFF, because of the nonlinear and complex behavior of material in modeling and control. In this research a modeling platform was developed and implemented to show the module behavior after activation. Furthermore, the modeling platform was used in simulation to develop a proper control algorithm.

Position control of the module to a desired location was the goal. Because of the model complexity and weaknesses, model based controllers was not usable in practical applications. So, in this paper an experimental control policy was utilizes. Any desired set point in the workspace of the module was achieved using the controller with a reasonable accuracy. So, by connecting a number of modules together in series, a modular manipulator is achieved. A predefined shape is produced by the manipulator when setting a desired position for every module. Calculating the desired position of every module in modular manipulator is an inverse kinematic problem which was not under focus of this paper. Moreover the module is a proper joint and actuator at the same time for any continuum robotic arm especially in micro robotic applications. Such capability is very useful in developing continuum bio inspired manipulators.

The other attractive feature of the module is possibility of regulating stiffness in addition to position. In many applications, such as endoscopic manipulators, the rigidity or the softness of manipulator is as important as the position. By enhancing the control strategy, it is possible to control the contact force between the manipulator and environment. In the future works, a common modular manipulator will be developed. Further, simultaneous control of position and stiffness in the manipulator will be studied.

References

Abadie, J., Chaillet, N. and Lexcellent, C. (2009), "Modeling of a new SMA micro-actuator for active endoscopy applications", *Mechatronics*, **19**(4), 437-442.

Ashrafiuon, H. and Jala, V.R. (2009), "Sliding mode control of mechanical systems actuated by shape memory alloy", *J. Dyn. Syst. - T ASME*, **131**(1), 011010-6.

Brinson, L. (1993), "One-dimensional constitutive behavior of shape memory alloys: thermomechanical derivation with non-constant material functions and redefined martensite internal variable", *J. Intel. Mat. Syst. Str*., **4**(2), 229-242.

De Sars, V., Haliyo, S. and Szewczyk, J. (2010), "A practical approach to the design and control of active endoscopes", *Mechatronics*, 20(2), 251-264.

Gao, X., Qiao, R. and Brinson, L.C. (2007), "Phase diagram kinetics for shape memory alloys: a robust finite element implementation", *Smart Mater. Struct*., **16**(6), 2102-2115.

Hadi, A. (2012). "Modeling a flexible miniatur module actuated by shape memory alloys", *Proceedings of the International Conference on Automation, Mechatronics and Robotics*, Phuket, Aug.

Hadi, A., Yousefi-Koma, A., Moghaddam, M., Elahinia, M. and Ghazavi, A. (2010), "Developing a novel SMA-actuated robotic module", *Sensor. Actuat. A - Phys*., **162**, 72-81.

Jayender, J., Patel, R.V. and Nikumb, S. (2009), "Robot-assisted active catheter insertion: algorithms and experiments", *Int. J. Robot. Res*., **28**(9), 1101-1117.

Kai, Y. and Chenglin, G. (2007), "Research and application of entirely-integrated spatial-bending shape memory alloy actuator", *Proceedings of the International Conference on Electrical Machines and Systems*, Seoul, Oct.

Lagoudas, D.C. (2008), Shape Memory Alloys Modeling And Engineering Application, Springer.

Lagoudas, D.C. and Tadjbakhsh, I.G. (1992), "Active flexible rods with embedded SMA fibers", *Smart*

Mater. Struct., **1**(2), 162.
Lanteigne, E. and Jnifene, A. (2008), "An experimental study on a SMA driven pressurized hyper-redundant manipulator", *J. Intel. Mat. Syst. Str*., **19**(9), 1067-1076.
Liang, C. and Rogers C.A. (1990), "One-dimensional thermomechanical constitutive relations for shape memory materials", *J. Intel. Mat. Syst. Str*., **1**(2), 207-234.
Menciassi, A., Park, J.H. and Lee, S. (2002), "Robotic solutions and mechanisms for a semi-autonomous endoscope", P*roceedings of the IEEE/RSJ International Conference on Intelligent Robots and Systems*, Sep.
Mineta, T., Mitsui, T. and Watanabe, Y. (2001), "Batch fabricated flat meandering shape memory alloy actuator for active catheter", *Sensor. Actuat. A - Phys*., **88**(2), 112-120.
Mineta, T. and Mitsoui, T. (2002), "An active guide wire with shape memory alloy bending actuator fabricated by room temperature process", S*ensor. Actuat. A - Phys*., **97**, 632-637.
Peirs, J. and Reynaerts, D. (1998), "Design of a shape memory actuated endoscopic tip", *Sensor. Actuat. A - Phys*., **70**, 135-140.
Salari, N. and Asgarian, B. (2015), "Seismic response of steel braced frames equipped with shape memory alloy-based hybrid devices", *Struct. Eng. Mech*., **53**(5), 1031-1049.
Shu, S.G., Lagoudas, D.C., Hughes, D. and Wen, J. (1997), "Modeling of a flexible beam actuated by shape memory alloy wires", *Smart Mater. Struct*., **6**, 265-277.
Tanaka, K. (1986), "A thermomechanical sketch of shape memory effect: one-dimensional tensile behavior", *Res. Mechanica*, **18**, 251-263.
Zhou, X. and You, Z. (2015), "Theoretical analysis of superelastic SMA helical structures subjected to axial and torsional loads", *Smart Struct. Syst*., **15**(5), 1271-1291.

CC